Engineering Science and Technology, an International Journal 22 (2019) 794–800

HOSTED BY

Contents lists available at ScienceDirect

Engineering Science and Technology, an International Journal

journal homepage: www.elsevier.com/locate/jestch

Full Length Article

Dual fluoroscopic evaluation of human tibiofemoral joint kinematics during a prolonged standing: A pilot study

Sabri Uzuner [a,*], Marcel L. Rodriguez [b], LePing Li [b], Serdar Kucuk [c]

[a] Duzce University, Duzce, Turkey
[b] University of Calgary, Calgary, Canada
[c] Kocaeli University, Kocaeli, Turkey

ARTICLE INFO

Article history:
Received 31 July 2018
Revised 3 November 2018
Accepted 24 December 2018
Available online 7 January 2019

Keywords:
Creep
In vivo study
Knee joint kinematics
Dual fluoroscopy
Magnetic resonance imaging
Image-based computer model

ABSTRACT

A complete knowledge of tibiofemoral joint kinematics is essential for understanding the function of the healthy and pathological joint. The objective of the present study was to establish a dual fluoroscopic measurement protocol and a data processing approach for the creep response of the knee joint in order to further evaluate the mechanical properties of articular cartilage and meniscus in vivo. A computational approach was developed for the determination of 3D translations and rotations of the joints of young participants with no history of injury using dual fluoroscopic images of loaded joints and joint geometry reconstructed from magnetic resonance imaging of the unloaded joints. High-resolution X-ray images were obtained for the distal femur and proximal tibia during 10-min standing when approximately ¾ body weight was slowly applied to the right leg and then kept constant for the rest duration of the test. Anatomic coordinate systems were established for the 3D models of distal femur and proximal tibia. Translations and rotations of the joint as functions of time were then evaluated using the X-ray images and these coordinate systems with the JointTrack software. The displacements in the proximal-distal direction obtained from two participants were consistent, showing a substantial increase in the initial phase when joint loading increased from nil to ¾ body weight and a continued small increase over time while the joint loading remained constant. The maximum anterior-posterior translations during 10-min standing were approximately 4 mm for both participants, although one showed better stability than the other. In conclusion, a creep loading protocol of the knee joint can be reasonably established for in vivo conditions and evaluated with the image-based computational approach.

1. Introduction

It is essential to understand tibiofemoral (TF) joint kinematics in order to diagnose the early onset of osteoarthritis and develop relevant therapeutic or surgical treatments [1–3]. In addition, the results obtained from the kinematic analysis of the TF joint can be used in the finite element analysis to understand the contact mechanics of the tissues in the knee joint under loading. There exist many in-vitro cadaveric and in vivo human studies on TF joint kinematics in the literature. However, only a few of these studies have considered the physiological weight-bearing stance [4–10]. With the development of medical imaging systems such as magnetic resonance imaging (MRI), single-plane fluoroscopy, dual fluoroscopy (DF), and computed tomography (CT), in vivo TF joint kinematic analysis has received great attention [11–16]. As compared with in-vitro studies, the results obtained from in vivo TF joint kinematics studies may be more realistic and accurate, since there are no TF contact shifts with the intact ligaments and muscles [17].

There are two main approaches in in vivo TF joint kinematic analysis: marker-based and markerless. In marker-based approaches, markers mounted on the surface of the skin or subcutaneous bone are used for monitoring the bone movements in the

Abbreviations: TF, tibiofemoral (joint); DF, dual fluoroscopy; MRI, magnetic resonance imaging; CT, computed tomography; ML, medial-lateral (orientation); PD, proximal tibia-distal femur (orientation); AP, anterior-posterior (orientation); VV, valgus-varus (rotation); IE, internal-external (rotation); FE, flexion-extension (rotation).

* Corresponding author at: Mechatronics Department, Dr. Engin PAK Cumayeri Vocational School, University of Duzce, Mehmet Akif Mah. Cumhuriyet Cad. No: 71/A, Cumayeri, Düzce 81700, Turkey.

E-mail addresses: sabriuzuner@duzce.edu.tr (S. Uzuner), leping.li@ucalgary.ca (L. Li), skucuk@kocaeli.edu.tr (S. Kucuk).

Peer review under responsibility of Karabuk University.

https://doi.org/10.1016/j.jestch.2018.12.014
2215-0986/

TF joint [17–20]. The effect of soft tissue motion on joint kinematics must be mathematically corrected [21–24]. On the other hand, in markerless approaches, the kinematic analysis is not compromised by the soft tissue motion. In addition to their high accuracy and resolution, the markerless approaches necessitate less time to prepare the experimental setup and analyze the data [25]. One of the most widely employed systems in the markerless approaches is the high-speed and high-resolution DF system. Through a system of two x-ray sources and two cameras, DF provides the bone positions of the TF joint with x-ray images from two different angles [2,15,16,26], which can then be used to determine the translations and rotations of the bones in all 6 degrees of freedom. Although MRI and CT systems could also provide high spatial 3D tissue geometry, they have low temporal resolution [27,28]. On the other hand, a DF system combines high temporal with high spatial resolution to capture joint motion [29]. Thus, a DF system was employed in the present study to obtain the joint displacement as a function of time during a weight-bearing standing.

The time-dependent TF joint contact was measured previously by Hosseini and colleagues with two orthogonal fluoroscopes during 300-s creep when a full-body weight was applied in about one second [30]. The present study focused on the creep displacement instead of contact area of the joint. Therefore, we applied a partial body weight as slow as the participant can comfortably achieve and maintain an almost constant loading as long as possible during the measurement. A prolonged loading or creep phase may better demonstrate the nonlinear time-dependent behavior of the joint. Such loading protocols may be used to evaluate the mechanical properties of articular cartilage and meniscus in vivo or validate a computational joint model. The objective of the present study was to establish a dual fluoroscopy measurement protocol and a data processing approach for the creep response of the TF joint.

2. Material and methods

Two participants with no history of leg injury were recruited for the study, a 24-year-old female of 59 kg and a 25-year-old male of 68 kg. The right knee joints were imaged. The combined MRI and DF study was approved by the Conjoint Health Research Ethics Board at the University of Calgary, Canada. The procedure for the kinematic data acquisition of the TF joint of a human participant involves the following steps: (1) obtaining the MRI of the unloaded knee and the DF images of the knee joint and ground reactions of the foot during 10-min standing; performing an MRI reconstruction to build a 3D model of the joint; (2) calibrating and correcting the distorted DF images; (3) determining the anatomic coordinate systems for the femur and tibia; and (4) matching the 2D undistorted images with the 3D model to determine the bone displacement.

2.1. MRI and DF image acquisition

The MRI measurement was done on unloaded knees using a 3-Tesla MRI unit (GE 750, GE, USA) at Seaman Family MR Research Centre, Foothills Medical Centre at the University of Calgary. In order to ensure the residual deformation of cartilages and menisci at a minimum level prior to testing, either subject was taken from her/his residence by a car in the early morning to the hospital and then carried to the MRI center with a wheelchair. Furthermore, the participant remained seated in an MRI compatible wheelchair for at least 30 min prior to the MRI. She/he was then moved to the Clinical Movement Assessment Lab, which is in the same hospital with the MRI center, with a wheelchair for the DF measurement. The participant avoided loading her/his right leg until the DF measurement.

The MRI sequence was a high-resolution FIESTA scan of the TF joints including 20 cm above and below the joint line (Steady state free precision; Slice thickness: 1 mm; Field of view: 24×24 cm^2; 200 slices; Slice spacing: 0.5 mm; Matrix: 512×512 pixels). The images of the hip and ankle were also obtained but at lower resolution; they were used to identify the anatomical coordinate system for the femur and tibia [30]. MR images were transferred into AMIRA software (Thermo Fisher Scientific, Carlsbad, USA) for 3D model reconstruction of the knee joint. Segmentation and reconstruction of the female knee joint are demonstrated in Fig. 1.

DF imaging techniques were used to capture the six-degree-of-freedom kinematics of the TF joints during 10-min standing after a partial body weight was slowly applied in 5–7 s (Figs. 2 and 3). The DF system consists of two high-speed X-ray generators and two high-speed solid-state video cameras (Fig. 2). It is equipped with low dose X-ray technology and high frame rates (6–250 Hz), even its lowest imaging frequency would be more than adequate to provide the required temporal resolution to track the 3D translations

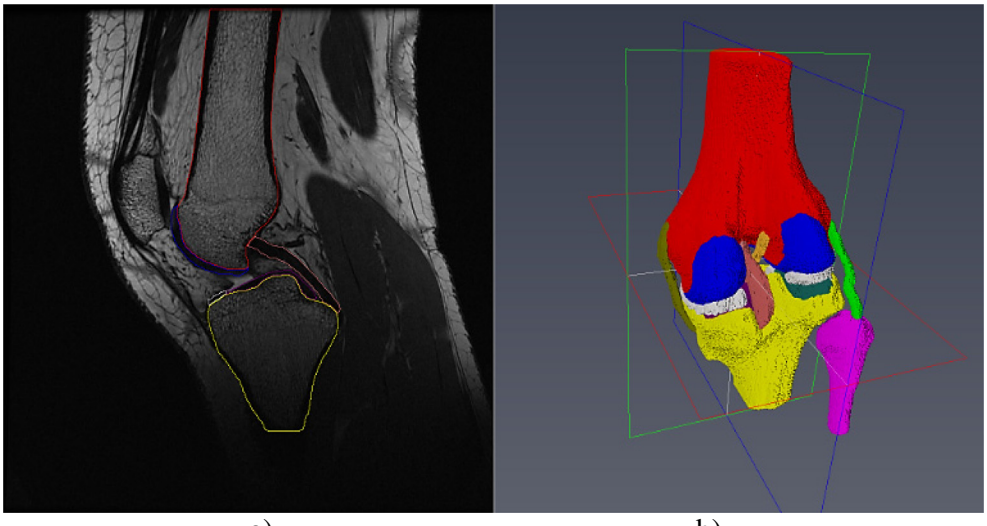

Fig. 1. Schematic representation of MRI reconstruction of the knee joint: a) Segmentation, b) Reconstruction of the 3D model.

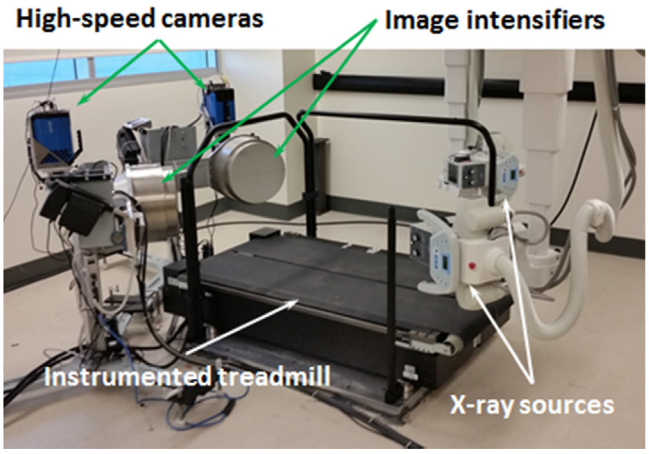

Fig. 2. Dual fluoroscopic imaging system at the Clinical Movement Assessment Lab.

and rotations of the bones of the TF joint during 10 min knee compression [31].

The loading protocol was tested beforehand without X-rays and found to be appropriate, as shown by the reaction forces measured by the instrumented treadmill. Braces were used to constrain the movement of the tested leg to full extension (Fig. 3b). The participant initially stood straight on her left leg with the aid of handrails. She then gradually applied her weight onto her right leg by slowly lowering her right foot to the treadmill floor but keeping her right leg and body straight (Fig. 3), during which time (5–7 s) the force in the right leg increased from nearly zero to approximately ¾ body weight. She then tried to balance herself to keep the force in the right knee unchanged for the rest duration of the test (10 min in total). We did not ask her to apply an exact amount of weight to the right leg, but the participant decided to stand still without shifting additional weight to the leg whenever she felt comfortable in her position.

It was reported in previous studies that the deformation rate of soft tissues of TF joints was high during the loading phase but decreased rapidly after the first minute [30]. In this context, in order to track the translations and rotations of bones of the joints precisely and, in the meantime, minimize the amount X-rays to the participants, DF images were acquired from the cameras at a frame rate of 6 Hz, continuously for the first minute, and at 6 Hz for 2 s intermittently with 28-s breaks for the rest nine minutes. A total of 563 pairs of images with high-resolution were thus taken by the two cameras.

2.2. Image calibration

By nature of the imaging process, the DF images are distorted because of the structure of camera lens and the distance of the object to the cameras. Therefore, these images need to be corrected so that the TF joint kinematics can be obtained accurately from the undistorted images. An acrylic cubic calibration frame was used as a reference, and an algorithm previously developed by Lichti and colleagues [31] with MATLAB software (The MathWorks Inc., Version R2017a, Natick, MA, USA) was employed for the image calibration. The calibration frame enables the acquisition of external and internal parameters of the system for the imaging data correction using a self-calibrating bundle adjustment method [14]. This method has been proven to be of high accuracy and efficiency as compared to other calibration approaches such as a two-step direct linear transform method [31].

2.3. Determination of the coordinate systems for femur and tibia

The purpose of establishing the coordinate systems is to allow us to calculate the absolute and relative positions of the femur and tibia and to determine the position changes over time. The coordinate systems of the femur and tibia (Fig. 4) were to be determined using the anatomy of the leg reconstructed from the MRI [32]. In this context, the coordinate systems characterize the specific knee joint and describe the joint motion, i.e. three relative translations and three relative rotations (proximal–distal (PD), anterior-posterior (AP), medial–lateral (ML), valgus-varus (VV), internal-external (IE), and flexion–extension (FE)).

The coordinate systems for the knee joint were determined using the 3D models of the knee, hip and ankle from MRI reconstruction (Fig. 4). The long axes for the femur and tibia were obtained through a MATLAB procedure developed by Sharma and colleagues [14], which makes use of the point clouds selected according to the anatomy of femur, hip, tibia and ankle (Fig. 5). The point cloud selection process was conducted through open-source ParaView software (BSD, Kitware Inc, NM, USA). The procedure creates the coordinate system for each bone, as described as follows. For the femur, two spheres are placed, respectively, in the medial and lateral condyles, and an ML line is obtained by joining the centers of the spheres [33]. The center of the ML line is then

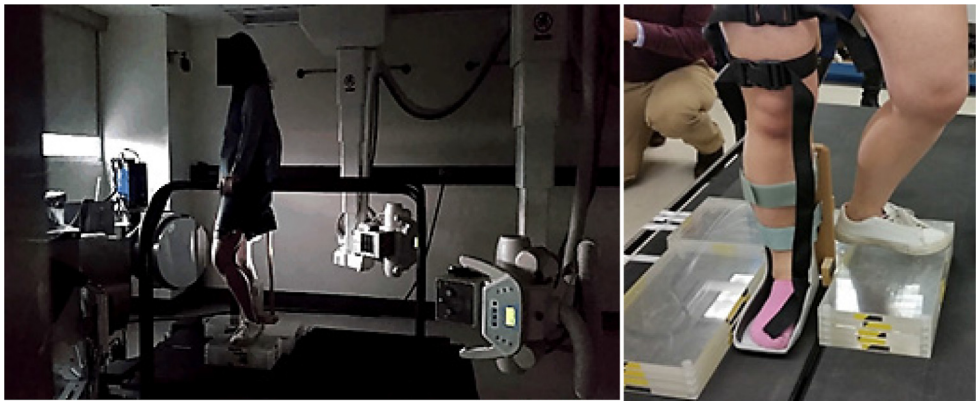

a) b)

Fig. 3. Dual fluoroscopic measurement of the right knee: a) The right leg is loaded with approximately 3/4 body weight in full extension during 10 min standing; b) A brace was used to minimize the flexion and rotation of the bones of the TF joint. The participant wore a lead apron during a test (photos shown were taken during a rehearsal without the lead apron).

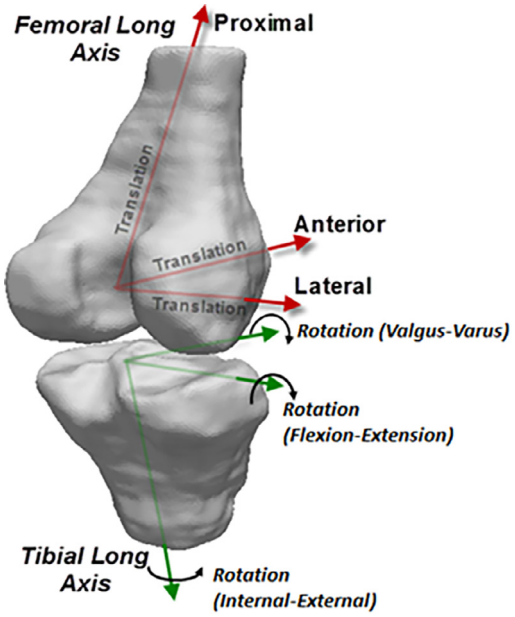

Fig. 4. Anatomic coordinate systems of the femur and tibia based on the anatomy of the leg.

selected as the origin of the coordinate system of the femur with the lateral axis aligning with the ML line (Fig. 5). The long axis of the femur overlaps the PD line which is the line from the origin to the spherical center of the hip. Finally, the cross-product of the PD and ML axes determines the AP axis, shown in Fig. 4 as anterior axis. A similar procedure can be performed on the proximal tibia and ankle to obtain the long axis of the tibia [14,32].

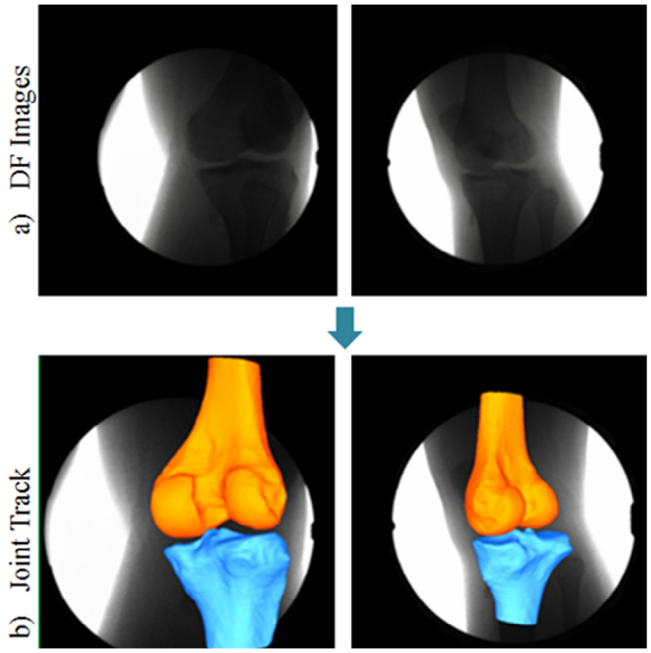

Fig. 6. The 2D-3D matching process for the female participant: a) Corrected DF images of the knee joint obtained during 10 min standing; b) Markerless 2D–3D registration of 3D bones with pairs of corrected DF images.

2.4. 2D-3D matching process

JointTrack Biplane software (University of Florida, Gainesville, FL, USA) was used to match the 3D model of the femur and tibia with the 2D undistorted images. The software calculates and

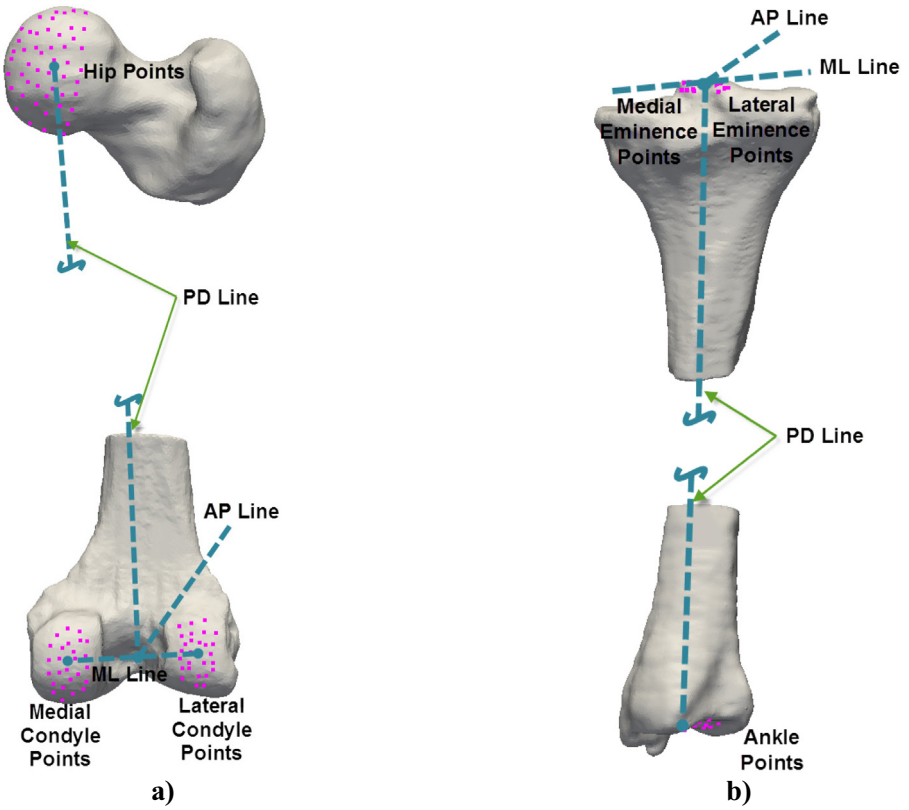

Fig. 5. The anatomic coordinate systems established using point clouds with ParaVIEW: a) the coordinate system for the femur; b) the coordinate system for the tibia. (PD = proximal–distal).

reports the 3D motions of bones through the matching process until the silhouette of bones provides an optimal fit with the 2D undistorted images that have been computationally obtained from the initially distorted DF images (Fig. 6).

Cameras placed at different angles in the DF system provide two images of the same bones of the TF joint from different angles for any given time through two X-ray sources. In this way, data of 3D position of the bones are acquired through these 2D images. The silhouette of the bone was overlaid manually on the two undistorted images. This process was repeated meticulously, taking 56 and 61 pairs of samples from all 563 pairs of images obtained for the female and the male participants, respectively. The samples were taken at 1–2-s intervals for the first minute to capture the fast motion of bones during the loading and early creep phases, and at 30 s intervals for the rest nine minutes of slow motion. This sampling approach was found to be sufficient to obtain the time-dependent translations and rotations of the bones for the 10-min standing.

The results obtained from the JointTrack software are the absolute motions of the femur and tibia with respect to their axes. A custom MATLAB code was thus prepared using the Euler Angles (ZYX sequence) equations [34] to obtain the relative motions between the femur and tibia from the absolute motions, as the relative motions are more relevant to the joint mechanics.

3. Results

The TF joint kinematics for the female participant is shown with its six degrees of freedom as functions of time (Fig. 7). These results are relative motions of the distal femur with respect to the proximal tibia. The maximum relative rotations were 1.2, 4.3 and 0.54 degrees, respectively, in the VV, IE and FE rotations. The maximum relative translations were 0.23, 1.84 and 1.32 mm, respectively, in the PD, AP and ML directions (Fig. 7).

4. Discussion and conclusion

The study objective was to establish a measurement protocol and a data processing approach for the creep response of the human knee joint in vivo. A creep loading protocol was thus developed with standing weight bearing and tested on two participants (Fig. 8a, b). The images and results indicated the validity of the measurement and computer methods, although more measurements must be performed to gain confidence in the creep data. The creep displacement developed rapidly during the first minute, which is consistent with a similar study when the full body weight was applied in about one second and creep data were acquired for 300 s [30]. The loading rate used in the present study was much lower (~75%/6s = 12.5%/s as compared to 100%/s), and the creep

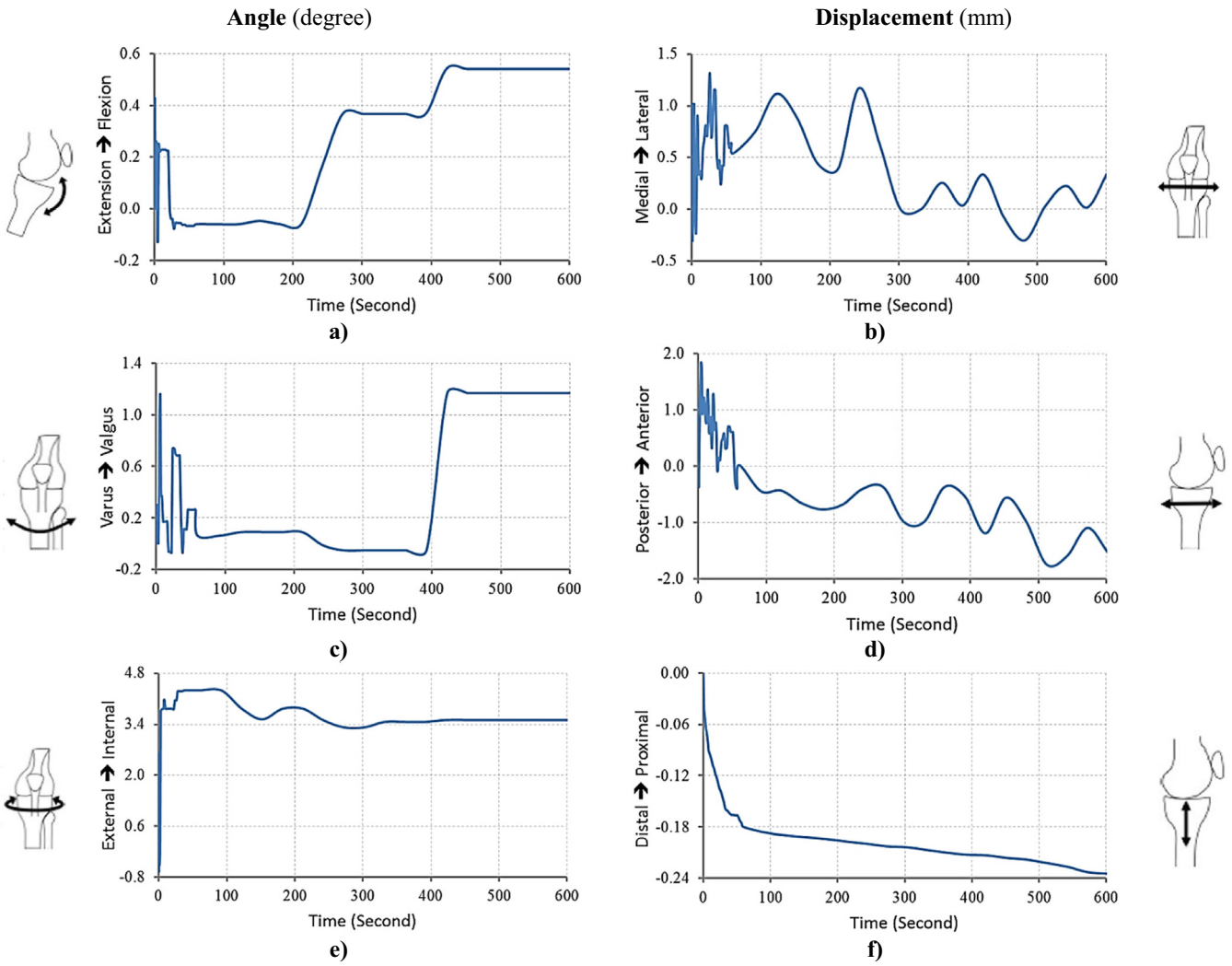

Fig. 7. The 3D relative motion of the TF joint for the female participant during 10 min standing with approximately 3/4 body weight: a, c & e) relative rotation of the femur with respect to the tibia; b, d & f) relative displacement of the femur with respect to the tibia.

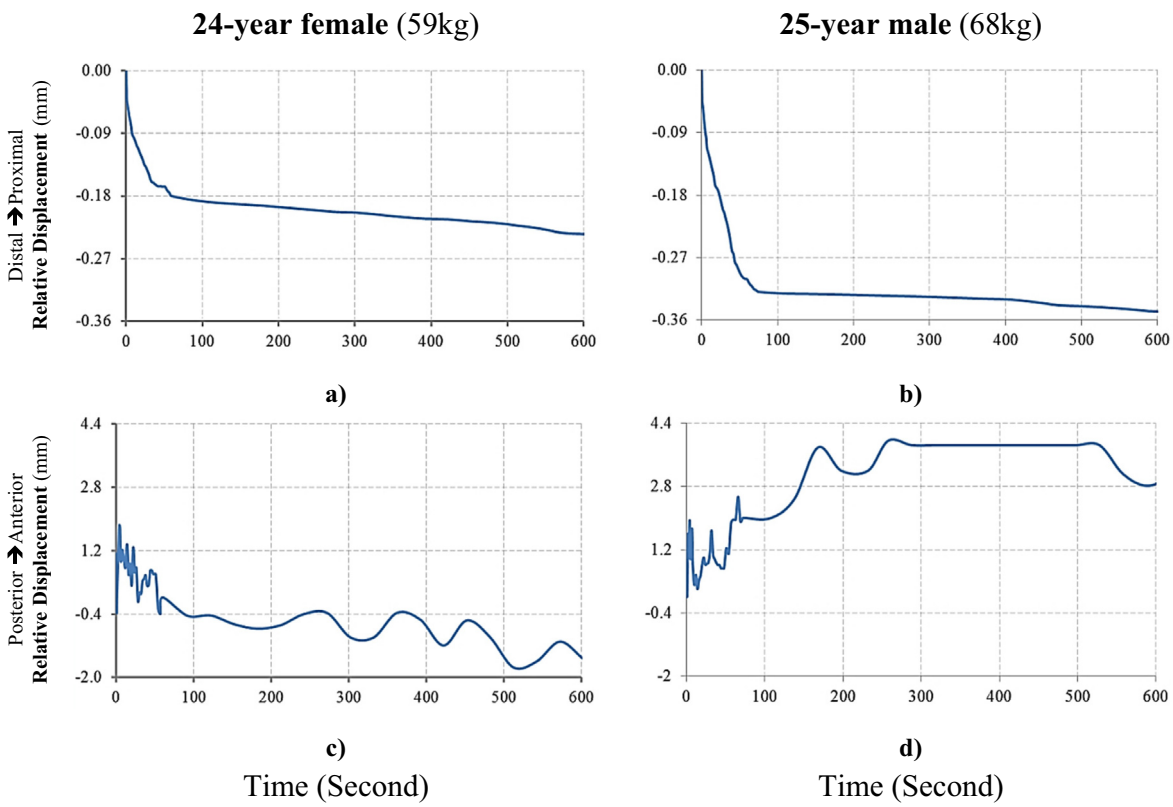

Fig. 8. Comparison of the TF joint kinematics for the female and male participants during the 10-min creep with approximately 3/4 body weight: a) & b) the relative displacement in the PD translation; c) & d) the relative displacement in the AP translation.

test was extended to 600 s. The extended loading phase may be better used to evaluate the nonlinear properties of the tissues in vivo, and the prolonged creep phase may be used to estimate multiple characteristic times of the tissues, as the short-term response is mainly determined by the fast spectrum of the time dependence.

Both participants applied approximately ¾ body weight to the tested legs, although there was no control on the load application. The participants were only expected to apply slightly more than half the body weight. However, this result was reasonable because their left legs were higher and bent to reduce the rotations of the right legs during the load application.

A creep test of the human knee joint in vivo can be possibly performed with participants using the partial bodyweight as loading, as demonstrated by the vertical displacement (Fig. 8a & b; force curve not included). However, the transverse displacements and rotations of the joint were difficult to control (Fig. 7a–e). Interestingly, the maximum change in AP translation during the 10 min standing was approximately 4 mm for both participants (Fig. 8c & d). Furthermore, the femur of both participants generally moved in one direction with respect to the tibia. However, the male participant seemed to have better motion control than the female on both AP (Fig. 8d vs c) and ML translations (the latter not included), possibly because he regularly played volleyball and had better knee stability from the muscles. This is supported by the finding that athletes may maintain a more stable stance than non-athletes during one-legged stances [35].

Creep of the knee joint would definitely take more than 600 s to complete (Fig. 8a, b), although the contact area was reported to remain constant after 50 s [30]. The two findings may be consistent with each other because the distance between the proximal tibia and distal femur can be further reduced after the contact in the knee has almost reached its maximum. Our finding is consistent with specimen testing [36], porcine joint testing [37] and previous human knee joint modeling [38], where a creep test takes at least an hour to reach a complete equilibrium.

In addition to the poor control on the transverse displacements and rotations of the joint, a major limitation of this study is the manual 2D-3D matching process with the JointTrack software. Because of human factors, it is difficult to foresee the errors in this matching process. For this reason, the quantitative results may need to be verified with further studies. Alternatively, the measurement and data processing approaches developed in the present study may be further tested with femoral and tibial prostheses of known geometry [14]. The general methods used in this study were validated in previous studies [14,15].

The data obtained from the combined MRI and DF measurements will be used to validate and refine a viscoelastic poromechanical model developed previously [38]. A validated model can be used to understand joint injuries and cartilage mechanobiology in vivo. On the other hand, the present study may be used to evaluate the properties of cartilage and meniscus in vivo in order to determine early tissue degeneration, when the data obtained from measurements are further interpreted with a finite element analysis.

In summary, dual fluoroscopic images of the knee joint were used to determine the kinematics of the tibiofemoral joint of human participants during a prolonged standing weight-bearing task. The 3D motion of the bones was found when comparing the undistorted 2D images with the 3D models of the distal femur and proximal tibia reconstructed from magnetic resonance imaging. The prolonged standing reasonably approximates a creep response of the joint and may be used to evaluate the mechanical properties of cartilage and meniscus in vivo using a validated computational model of the joint.

Acknowledgments

We greatly appreciate the help of Dr. Janet Ronsky, Dr. Gregor Kuntze and Ms. Jessica Kupper with the DF measurement and processing at the Clinical Movement Assessment Lab, University of Calgary.

We would also like to especially thank TUBITAK (The Scientific and Technological Research Council of Turkey) for the financial and moral support of Sabri Uzuner's visit to the University of Calgary. This research was funded by the Natural Sciences and Engineering Research Council of Canada.

A short version of this paper was published in the proceedings of ICATCES 2018.

The study was approved by the Conjoint Health Research Ethics Board at the University of Calgary, Ethics ID REB15-1165. The X-ray exposure for a participant of the present study was estimated to be 0.21 mSv.

References

[1] D. Paley, Normal lower limb alignment and joint orientation, in: Principles of Deformity Correction, Springer, Berlin, Heidelberg, 2002, pp. 1–18.
[2] K.M. Varadarajan, T.J. Gill, A.A. Freiberg, H.E. Rubash, G. Li, Gender differences in trochlear groove orientation and rotational kinematics of human knees, J. Orthop. Res. 27 (7) (2009) 871–878.
[3] F. Liu, M. Kozanek, A. Hosseini, S.K. Van de Velde, T.J. Gill, H.E. Rubash, G. Li, In vivo tibiofemoral cartilage deformation during the stance phase of gait, J. Biomech. 43 (4) (2010) 658–665.
[4] T. Siebel, W. Kafer, In vitro investigation of knee joint kinematics following cruciate retaining versus cruciate sacrificing total knee arthroplasty, Acta Orthopaedica Belgica. 69 (5) (2003) 433–440.
[5] G. Li, S. Zayontz, L.E. DeFrate, E. Most, J.F. Suggs, H.E. Rubash, Kinematics of the knee at high flexion angles: an in vitro investigation, J. Orthop. Res. 22 (1) (2004) 90–95.
[6] T. Fukubayashi, P. Torzilli, M. Sherman, R. Warren, An in vitro biomechanical evaluation of anterior-posterior motion of the knee. Tibial displacement, rotation, and torque, J. Bone Joint Surgery. Am. vol. 64 (2) (1982) 258–264.
[7] A. Garg, P. Walker, Prediction of total knee motion using a three-dimensional computer-graphics model, J. Biomech. 23 (1) (1990) 45–58.
[8] K.G. Nilsson, J. Kärrholm, L. Ekelund, Knee motion in total knee arthroplasty. A roentgen stereophotogrammetric analysis of the kinematics of the Tricon-M knee prosthesis, Clin. Orthop. Relat. Res. 256 (1990) 147–161.
[9] K.G. Nilsson, J. Kärrholm, P. Gadegaard, Abnormal kinematics of the artificial knee: roentgen stereophotogrammetric analysis of 10 Miller-Galante and five New Jersey LCS knees, Acta Orthopaedica Scandinavica. 62 (5) (1991) 440–446.
[10] A.A. Amis, W. Senavongse, A.M. Bull, Patellofemoral kinematics during knee flexion-extension: an in vitro study, J. Orthop. Res. 24 (12) (2006) 2201–2211.
[11] D.A. Dennis, R.D. Komistek, W.A. Hoff, S.M. Gabriel, In vivo knee kinematics derived using an inverse perspective technique, Clin. Orthop. Relat. Res. 331 (1996) 107–117.
[12] D.K. Ramsey, P.F. Wretenberg, Biomechanics of the knee: methodological considerations in the in vivo kinematic analysis of the tibiofemoral and patellofemoral joint, Clin. Biomech. 14 (9) (1999) 595–611.
[13] G. Li, L.E. DeFrate, H.E. Rubash, T.J. Gill, In vivo kinematics of the ACL during weight-bearing knee flexion, J. Orthop. Res. 23 (2) (2005) 340–344.
[14] G. Sharma, S. Saevarsson, S. Amiri, S. Montgomery, H. Ramm, D. Lichti, R. Lieck, S. Zachow, C. Anglin, Radiological method for measuring patellofemoral tracking and tibiofemoral kinematics before and after total knee replacement, Bone Joint Res. 1 (10) (2012) 263–271.
[15] G.B. Sharma, G. Kuntze, D. Kukulski, J.L. Ronsky, Validating dual fluoroscopy system capabilities for determining in-vivo knee joint soft tissue deformation: a strategy for registration error management, J. Biomech. 48 (10) (2015) 2181–2185.
[16] B. Ritchie, G. Kuntze, G. Sharma, J. Beveridge, J. Kupper, J. Ronsky, 2016. Determining in-vivo human tibiofemoral cartilage stiffness using dual fluoroscopy and magnetic resonance imaging. CMBES Proceedings. 39(1): Calgary, Alberta, Canada, May 24-27, 2016.
[17] M. Sati, J.A. de Guise, S. Larouche, G. Drouin, Improving in vivo knee kinematic measurements: application to prosthetic ligament analysis, Knee 3 (4) (1996) 179–190.
[18] M.S. Andersen, D.L. Benoit, M. Damsgaard, D.K. Ramsey, J. Rasmussen, Do kinematic models reduce the effects of soft tissue artefacts in skin marker-based motion analysis? An in vivo study of knee kinematics, J. Biomech. 43 (2) (2010) 268–273.
[19] D.L. Benoit, M. Damsgaard, M.S. Andersen, Surface marker cluster translation, rotation, scaling and deformation: their contribution to soft tissue artefact and impact on knee joint kinematics, J. Biomech. 48 (10) (2015) 2124–2129.
[20] Y. Wen, H. Huang, Y. Yu, S. Zhang, J. Yang, Y. Ao, S. Xia, Effect of tibia marker placement on knee joint kinematic analysis, Gait & Posture. 60 (2018) 99–103.
[21] A. Cappello, A. Leardini, F. Catani, P. La Palombara, Selection and validation of skin array technical references based on optimal rigid model estimation, Proc III Int Symp on 3-D Analysis of Hum Mov, 1994.
[22] E. Szczerbik, M. Kalinowska, The influence of knee marker placement error on evaluation of gait kinematic parameters, Acta Bioeng. Biomech. Wroc Univ. Technol. 13 (2011) 43–46.
[23] T.Y. Tsai, T.W. Lu, M.Y. Kuo, C.C. Lin, Effects of soft tissue artifacts on the calculated kinematics and kinetics of the knee during stair-ascent, J. Biomech. 44 (6) (2011) 1182–1188.
[24] J. Clément, R. Dumas, N. Hagemeister, J.A. De Guise, Soft tissue artifact compensation in knee kinematics by multi-body optimization: performance of subject-specific knee joint models, J. Biomech. 48 (14) (2015) 3796–3802.
[25] M.A. Perrott, T. Pizzari, J. Cook, J.A. McClelland, Comparison of lower limb and trunk kinematics between markerless and marker-based motion capture systems, Gait Posture 52 (2017) 57–61.
[26] J.-S. Li, T.-Y. Tsai, S. Wang, P. Li, Y.-M. Kwon, A. Freiberg, H.E. Rubash, G. Li, Prediction of in vivo knee joint kinematics using a combined dual fluoroscopy imaging and statistical shape modeling technique, J. Biomech. Eng. 136 (12) (2014) 124503.
[27] C. Peterfy, G. Gold, F. Eckstein, F. Cicuttini, B. Dardzinski, R. Stevens, MRI protocols for whole-organ assessment of the knee in osteoarthritis, Osteoarthritis and Cartilage. 14 (2006) 95–111.
[28] T. Mosher, E. Walker, J. Petscavage-Thomas, A. Guermazi, Osteoarthritis year 2013 in review: imaging, Osteoarthritis Cartilage 21 (10) (2013) 1425–1435.
[29] E.L. Brainerd, D.B. Baier, S.M. Gatesy, T.L. Hedrick, K.A. Metzger, S.L. Gilbert, J.J. Crisco, X-ray reconstruction of moving morphology (XROMM): precision, accuracy and applications in comparative biomechanics research, J. Exp. Zool. Part A: Ecol. Integrative Physiol. 313 (5) (2010) 262–279.
[30] A. Hosseini, S.K. Van de Velde, M. Kozanek, T.J. Gill, A.J. Grodzinsky, H.E. Rubash, G. Li, In-vivo time-dependent articular cartilage contact behavior of the tibiofemoral joint, Osteoarthritis Cartilage 18 (7) (2010) 909–916.
[31] D.D. Lichti, G.B. Sharma, G. Kuntze, B. Mund, J.E. Beveridge, J.L. Ronsky, Rigorous geometric self-calibrating bundle adjustment for a dual fluoroscopic imaging system, IEEE Trans. Med. Imaging 34 (2) (2015) 589–598.
[32] E.S. Grood, W.J. Suntay, A joint coordinate system for the clinical description of three-dimensional motions: application to the knee, J. Biomech. Eng. 105 (2) (1983) 136–144.
[33] F. Iranpour, A.M. Merican, W. Dandachli, A.A. Amis, J.P. Cobb, The geometry of the trochlear groove, Clin. Orthop. Relat. Res. 468 (3) (2010) 782–788.
[34] B. Siciliano, L. Sciavicco, L. Villani, G. Oriolo, in: Robotics: Modelling, Planning and Control, Springer Science & Business Media, 2010, p. 52.
[35] S. Matsuda, S. Demura, M. Uchiyama, Centre of pressure sway characteristics during static one-legged stance of athletes from different sports, J. Sports Sci. 26 (7) (2008) 775–779.
[36] V.C. Mow, S. Kuei, W.M. Lai, C.G. Armstrong, Biphasic creep and stress relaxation of articular cartilage in compression: theory and experiments, J. Biomech. Eng. 102 (1) (1980) 73–84.
[37] M.L. Rodriguez, L.P. Li, Compression-rate-dependent nonlinear mechanics of normal and impaired porcine knee joints, BMC Musculoskeletal Disorders 18 (2017) 447, https://doi.org/10.1186/s12891-017-1805-9.
[38] M. Kazemi, L.P. Li, A viscoelastic poromechanical model of the knee joint in large compression, Med. Eng. Phys. 36 (8) (2014) 998–1006.